Prince JA, Bhuvana S, Anbharasi V, Ayyanar N, Boodhoo KVK, Singh G.
Ultra-wetting graphene-based PES ultrafiltration membrane – A novel approach for successful oil-water separation.
***Water Research* 2016, 130, 311-318.**

Accepted Manuscript

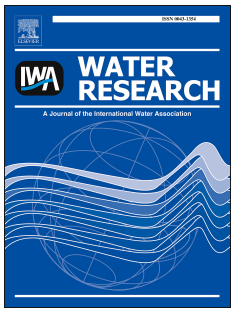

Ultra-wetting graphene-based PES ultrafiltration membrane – A novel approach for successful oil-water separation

J.A. Prince, S. Bhuvana, V. Anbharasi, N. Ayyanar, K.V.K. Boodhoo, G. Singh

PII: S0043-1354(16)30554-1

DOI: 10.1016/j.watres.2016.07.042

Reference: WR 12237

To appear in: *Water Research*

Received Date: 14 March 2016

Revised Date: 14 July 2016

Accepted Date: 18 July 2016

Please cite this article as: Prince, J.A., Bhuvana, S., Anbharasi, V., Ayyanar, N., Boodhoo, K.V.K., Singh, G., Ultra-wetting graphene-based PES ultrafiltration membrane – A novel approach for successful oil-water separation, *Water Research* (2016), doi: 10.1016/j.watres.2016.07.042.

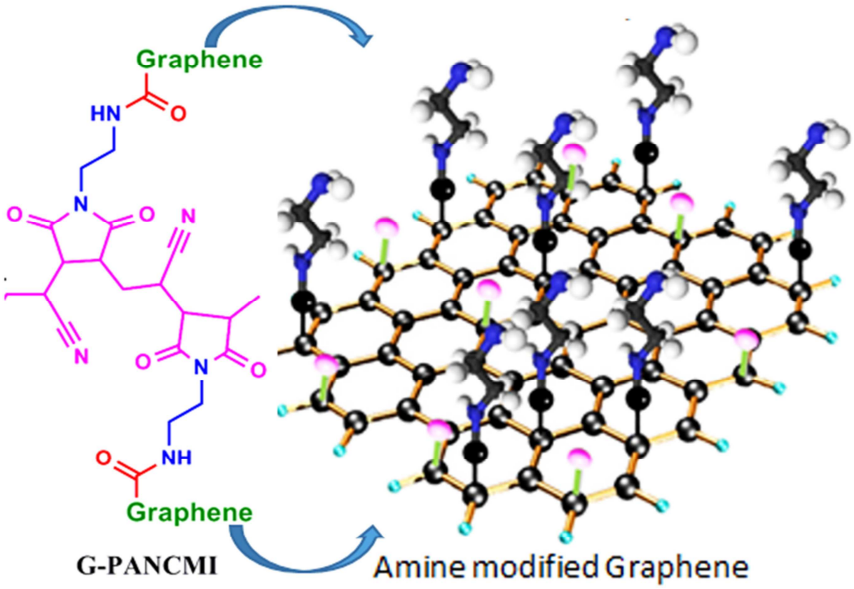

Ultra-wetting graphene-based PES ultrafiltration membrane - A novel approach for successful oil-water separation

J. A. Prince [a,b,], S. Bhuvana [a], V. Anbharasi [a], N. Ayyanar [a], K.V.K. Boodhoo[b] and G. Singh [a,]*

[a] Environmental & Water Technology – Centre of Innovation, Ngee Ann Polytechnic, Singapore 599489

[b] School of Chemical Engineering and Advanced Materials, Faculty of Science, Agriculture and Engineering, Newcastle University, Newcastle upon Tyne, NE1 7RU, United Kingdom

*Email: jap2@np.edu.sg

Keywords: (Ultra-wetting graphene, hydrophilicity, ultrafiltration, oil-water separation)

ABSTRACT:

Oil pollution in water and separation of oil from water are receiving much attention in recent years due to the growing environmental concerns. Membrane technology is one of the emerging solutions for oil-water separation. However, there is a limitation in using polymeric membrane for oil water separation due to its surface properties (wetting behaviour), thermal and mechanical properties. Here, we have shown a simple method to increase the hydrophilicity of the polyethersulfone (PES) hollow fiber ultrafiltration (UF) membrane by using carboxyl, hydroxyl and amine modified graphene attached poly acrylonitrile-co-maleimide (G-PANCMI). The prepared membranes were characterized for its morphology, water and oil contact angle, liquid entry pressure of oil (LEP_{oil}), water permeability and finally subjected to a continuous 8 hrs filtration test of oil emulsion in water. The experimental data indicates that the G-PANCMI play an important role in enhancing the hydrophilicity, permeability and selectivity of the PES membrane. The water contact angle (CA_w) of the PES membrane is reduced from 63.7± 3.8^o to 22.6 ± 2.5^o which is 64.5% reduction while, the oil contact angle was increased from 43.6 ± 3.5^o to 112.5 ± 3.2^o which is 158% higher compared to that of the PES membrane. Similarly, the LEP_{oil} increased 350% from 50±10 kPa of the control PES membrane to 175± 25 kPa of PES-G-PANCMI membrane. More importantly, the water permeability increased by 43% with >99% selectivity. Based on our findings we believe that the development of PES-G-PANCMI membrane will open up a solution for successful oil-water separation.

1.Introduction

In recent years, oil-water separation is receiving much attention due to the growing environmental concerns related to oil pollution in water (Shannon, 2008). Large volumes of oil polluted wastewater are produced in various industries such as oil fields, metallurgical, petrochemical, pharmaceutical etc., in the form of oil water emulsion (Sirivedhin and Dallbauman, 2004). The untreated oil polluted wastewater contains harmful chemicals and dissolved minerals which are classified as hazardous waste and these will bring a negative impact on people's health and even will have damaging impact on the ecosystem and hence, governmental regulation are increasingly more stringent to remove the hazardous waste before discharge (Reilly et al., 1991; Group 1998).

The conventional oil-water separation techniques such as gravity separation, skimming and flotation are useful for free oil/water mixtures (Oil droplet >150µm and dispersed oil size range of 20-150 µm), but are not applicable to small size (<20µm) oil/water emulsions (Cheryan et al., 1998; Nordvik et al., 1996). Low efficiency and high operation cost are the other limiting factors of the conventional oil-water separation techniques. Therefore, advanced techniques are urgently needed to effectively separate various oil/water mixtures.

There is a growing tendency to use membrane technology for oil/water separation. Currently, there are two different types of membrane are in use for oil-water separation based on their surface properties. The first type is super hydrophobic-superoleophilic (Deng et al.,, 2013), these membranes are favourable for the oil transportation while repel the liquid water entering the pores. For example, silicon oxycarbide fibres (Lu et al.,, 2009), PTFE coated mesh (Feng et al., 2004), and modified polyester textile (Zhang and Seeger 2011). Membranes with rationally controlled pore size (to be smaller than the emulsified water droplets) are also suitable for effective oil-water separation (Zhang et al., 2013; Shi et al., 2013).

The second type is super hydrophilic-super-oleophobic (Xu et al., 2013). These membranes are favourable for the water transportation while repel the oil entering the pores. For example, aligned

ZnO nanorod array coated mesh (Tian et al., 2012), Zeolite-coated mesh (Wen et al., 2013), Alumina nanoparticles coated fabric (Samuel et al., 2011) and hydrogel-coated mesh are super hydrophilic in nature (Xue et al., 2011). The first type super hydrophobic-super oleophilic membrane has several drawbacks such as the adherence of high viscous oil to the membrane surface which is generally difficult to be removed and requires more chemical usage to remove it (Chen et al., 2013). The second type super hydrophilic-super oleophobic membranes are advantageous over the first type super hydrophobic-super oleophilic membranes. Because, these membranes allow only water to pass through, which reduces the possibility of membrane clogging. Similarly, they prevent the formation of water barrier between the membrane surface and the oil phase due to the fact that water is heavier than oil phase (Zhang et al., 2013).

Fig.1. shows how the water barrier affects the permeate flux in the first type super hydrophobic-super oleophilic membranes. For the first type super hydrophobic-super oleophilic membranes, the system has to operate in very high turbulent flow to push the oil emulsion towards the membrane. But, this process will increase the overall energy consumption of the system.

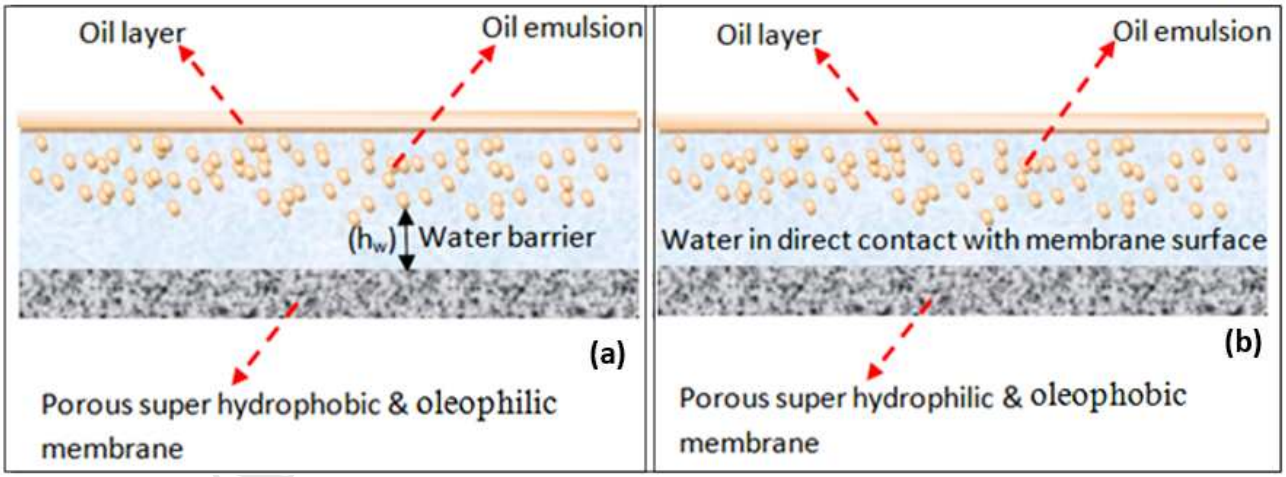

Fig. 1. a) Water in direct contact with membrane surface in the first type super hydrophobic-super oleophilic membranes, b) water barrier between the membrane surface and the oil emulsion in the second type super hydrophilic-super oleophobic membranes.

Generally, hydrophilic membrane exhibits an affinity for water. It possess a high surface energy value and has the ability to form hydrogen-bonds with water. Hydrophilic surface will repel the hydrophobic oily particles such as hydrocarbons, surfactants, grease etc. Recently, considerable attention has been focused to improve the surface hydrophilicity of the membranes along with

generation of surface micro-nano structures for oil-water separation, which results in super oleophobic surfaces with low oil-adhesion (Zhu et al., 2013; Zhang et al., 2012; Kota et al., 2012). Recently, carbon-based nanomaterials such as graphene (Gai et al., 2014), graphene oxide (Zinadini et al., 2014), carbon nanotube (Duan, 2014) and fullerene (Tasaki et al., 2007) have gained much attention in the field of membrane science and engineering due to its high surface area, high mechanical strength and chemical stability. Graphene is a sp^2-hybridized two-dimensional carbon sheet (Novoselov, 2004). Incorporating graphene and its derivative graphene oxide in a polymer matrix have shown improved membrane performance (Jin, 2013; Akin et al., 2014; Heo et al., 2013; Han et al., 2013; Sun, 2013; Zhao, 2013) . However, graphite and graphene are generally hydrophobic in nature which limits their application in water filtration (Li et al., 2008).

Here we report a novel method to produce ultra-wetting graphene based membrane for successful oil water separation. Initially, the wettability of graphene was increased by amine and carboxyl functionalisation. Graphene was first carboxylated using highly concentrated acid mixture (hydrochloric acid and sulphuric acids). The carboxylic group was further modified to acid chloride. Finally the acid chloride modified graphene oxide was amine functionalised by using ethylene diamine. The functionalized graphene oxide was then attached to a highly hydrophilic water insoluble polymer (poly acrylonitrile co maleic anhydride). The graphene oxide grafted poly acrylonitrile co maleimide (G-PANCMI) was used to prepare the dope solution. The hollow fibre ultrafiltration membranes were prepared by dry wet spinning.

The prepared membranes were characterized using (FTIR) spectroscopy, Contact angle (CA), Tensile testing, Zetapotential (surface charge analyser), scanning electron microscopy (SEM), and the Porometer. Both control PES and modified G-PANCMI-PES membrane were tested for the oil entry pressure and clean water flux. Finally, all the prepared membranes were tested for oil water separation, permeability, selectivity and antifouling property in long term experiments at two different temperatures.

2. Experimental

2.1 Materials

Polyethersulfone (PES) k-3010 powder was purchased from Sumitomo chemicals pte ltd, Japan. Acrylonitrile, Maleic anhydride, dichloroethane and azobisisobutyronitrile (AIBN) were purchased from sigma Aldrich with 99% purity. High purity ethanol, Nitric acid (HNO_3), Sulphuric acid (H_2SO_4), thionyl chloride ($SOCl_2$) and DMAc (N-N-Dimethyl acetamide), were also purchased from Sigma Aldrich and used as received. Castrol brake fluid oil was purchased locally. The xGnP, exfoliated graphite nano platelets were purchased from XG Sciences. The oily waste water (oil emulsion) was prepared by constantly mixing 200ppm of the oil in DI water at 400rpm using a multi blade mechanical stirrer. The water used for the reaction was distilled and de-ionized (DI) with a Milli-Q plus system from Millipore, Bedford, MA, USA.

2.2. Synthesis of functionalised xGnP

About 1 gram of the pristine xGnP was initially treated with an excess of acid mixture (H_2SO_4/HNO_3, 3:1) to introduce the acid functionality on to the graphene surfaces. After successful oxidation, the functionalised graphene was centrifuged, filtered and washed with excess water until the pH of the wash water was neutral. After through drying, the acid functionalised xGnP was further refluxed with 150ml of thionyl chloride at 80^{O}C for 24 hours. The excess thionyl chloride after the reaction was filtered off and then about 150ml of ethylene diamine was added to the reaction vessel and continued to reflux for another 48hrs. The amine functionalised xGnP was finally separated out by centrifugation and washed with excess ethanol to remove the unreacted reagents and further with water (**Fig.2**). The detailed synthesis of ultra-wetting graphene has been discussed in our recent publication (Prince et al., 2016).

2.3. Synthesis of xGnP grafted PANCMI

As shown in our recent study (Prince et al., 2016), PANCMA was synthesised as per our previously reported procedure using azobisisobutyronitrile as an initiator. The synthesised PANCMA was allowed to react overnight with the amine functionalised xGnP in 500ml of DMAc.

Further, 100ml of toluene was added to the reaction mixture and refluxed at 110^{o}C for about 5 hours and the toluene was distilled off from the reaction vessel. The product in DMAc was poured into methanol to separate the product in polyamic acid form. This intermediate product was further subjected to thermal imidisation using a multistage heating of 200^{o}C for 2hours and finally at 260^{o}C for another 30 mins to obtain the final xGnP grafted PANCMI (G-PANCMI). **Fig. 3** shows the schematic representation of the G-PANCMI synthesis.

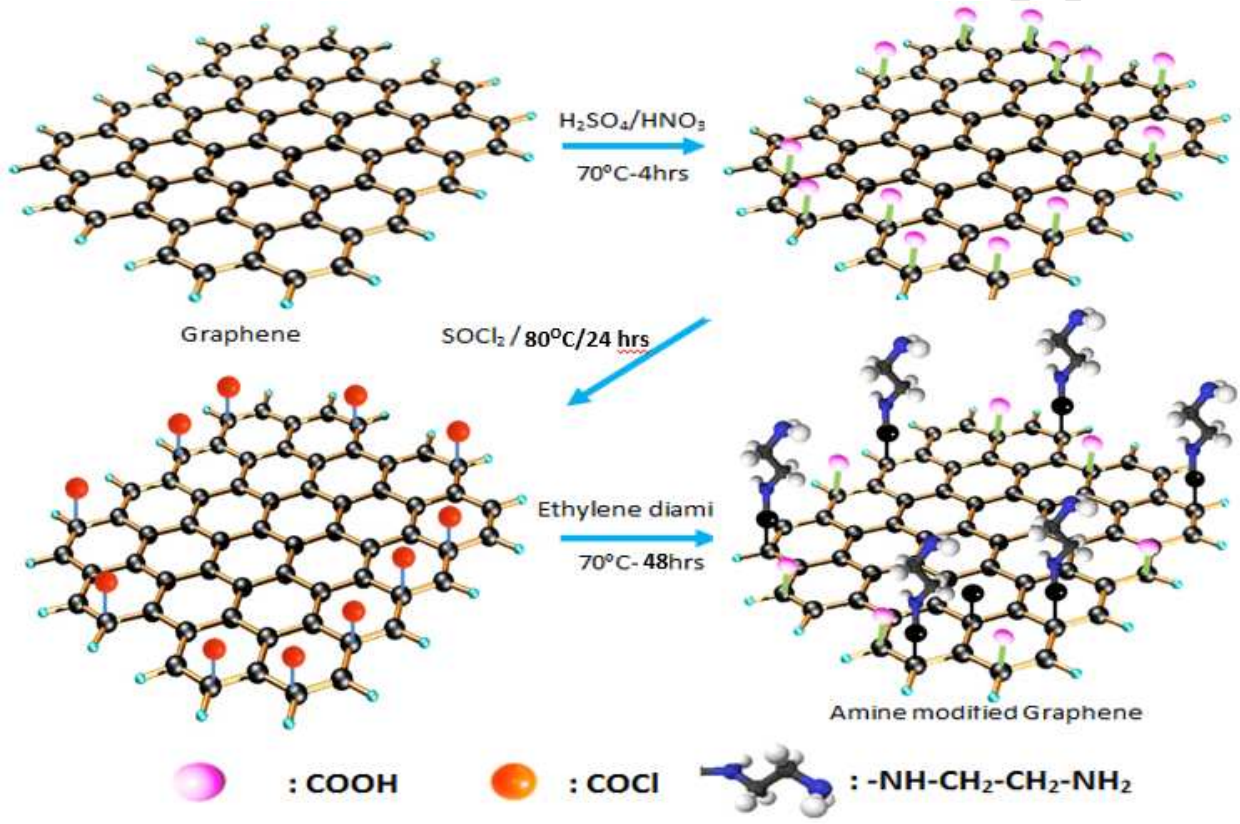

Fig. 2. Different steps involved in the amine functionalisation of xGnP

2.4 Fabrication of PES and PES-G-PANCMI hollow fibre membranes by dry wet spinning

The control Poly ether sulfone (PES) and xGnP grafted poly (acrylonitrile co maleimide) (G-PANCMI) modified PES-G-PANCMI hollow fibre ultrafiltration membranes were prepared by dry wet spinning method. PES was used as the base polymer, NMP was the base solvent, DEG was used as a non-solvent, PVP was used as an additive (pore forming agent) and G-PANCMI was used as a hydrophilic additive. Based on the results of our previous studies, the weight percentage of the polymeric additive to the PES dope was fixed as 5wt% (G-PANCMI)[34]. The

composition of the casting solution consists of 21 wt% PES, 5 wt% PVP-K-30, 5 wt% DEG, 69 wt% NMP respectively 5% of G-PANCMI was added to the PES-G-PANCMI dope composition by replacing 5% of NMP where the NMP concentration was 64%. The phase diagram of the dope compositions are presented in **Fig.4.** PVP powder was first added into the NMP /DEG mixture in a RB flask and the solution was stirred by a mechanical stirrer for at least 1-1.5 hours. After complete dissolution of PVP, PES and G-PANCMI were added and allowed to stir at a constant speed of 250~350 rpm for at least 24 h at 80^{o} C, to obtain a completely dissolved / dispersed homogeneous polymeric solution. The dope solution was poured into the polymer tank and degassed at a negative pressure of -0.6 bar for 15-20 min. Nitrogen gas was purged into the dope tank to create inert atmosphere and to push the polymer towards the polymer pump. NMP and water were mixed in 80:20 volume ratio **(N**MP: Water 80:20) was used as a bore liquid. The polymer solution and the bore liquid were pumped to the spinneret (OD 1.2 mm, ID 0.6 mm). The air gap was fixed at 50mm. The hollow fibre membranes were fabricated at around 25^{o} C and at around 65-70% relative humidity with a take up speed of 0.21 m/s. The membranes were then collected from the winder and left inside a water tank (post coagulation tank) for 24 hrs to washout the residual NMP, DEG and PVP that was not removed from the solution at the point of fabrication process. The membranes were immersed into a post treatment solution of 40% water and 60% glycerine before testing the clean water flux.

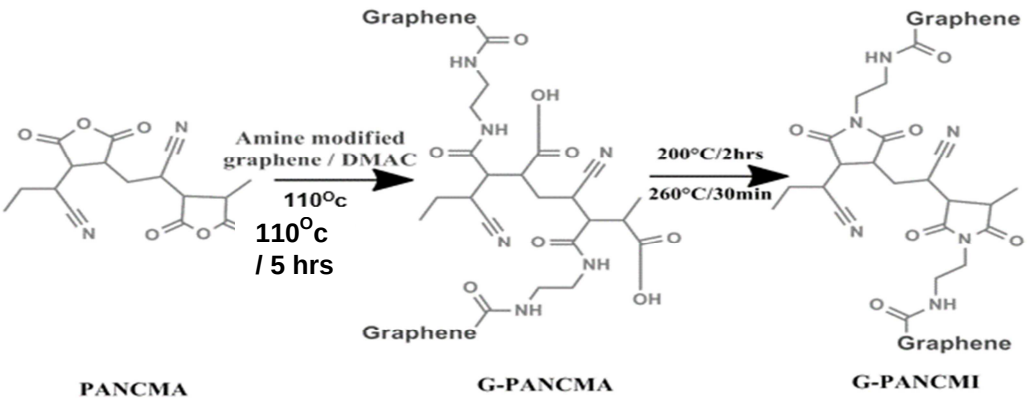

Fig. 3. Synthesis of xGnP grafted PANCMI

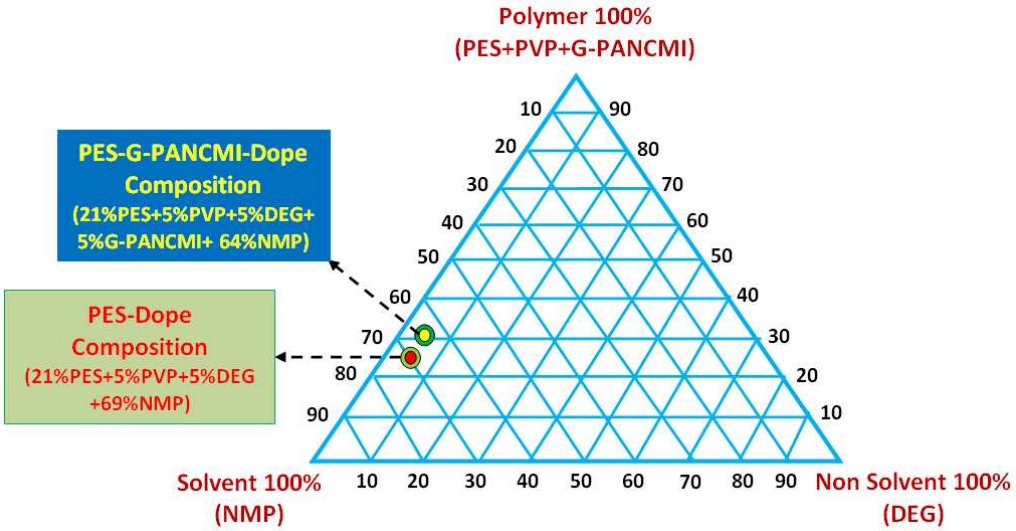

Fig.4. Phase diagram for the dope compositions

2.5 Characterization

A scanning electron microscope (SEM) Jeol Jsm-7600F coupled to a XmaxN detector for energy-dispersive X-ray (EDX) analysis was used to study the morphology and the overall chemical composition and the distribution of the chemical elements of interest in the membrane. The water contact angle (CAw) of the unmodified and modified hollow fibre membranes were determined using the Sigma 701 Tensiometer. Five readings were measured for each sample and an average was obtained from the results. The pore size of the membrane was measured using the Porometer 3G instruments (equipped with 3GWin control software) from Quanta chrome. Thermo gravimetric (TG) analysis of the samples (10-15mg) was performed on a Mettler-Toledo thermo gravimetric analyzer in temperature range of 30-500^{0}C with a heat ramping rate of 15°C min^{-1} under nitrogen atmosphere. The mechanical properties of the membranes were studied using an Instron universal materials testing machine (Model 3366). The hollow fibre samples (5 numbers) of length 100 mm were used for the test.

2.6 Liquid Entry Pressure experiment

The liquid entry pressure of oil (LEP_{oil}) was measured for the PES and PES-G-PANCMI membranes. 10 numbers of hollow fiber membranes of 30cm length were used to fabricate the

membrane module. The membrane modules were potted using epoxy glue to seal one side of the hollow fibers while keeping the other lumen side open to feed the liquid oil. The membrane module was kept in a non-pressured transparent box and the open lumen side of the membrane module was connected to the feed tank topped-up with oil (Castrol Brake Fluid Dot 4). Compressed nitrogen was used to apply pressure in the tank. The pressure was increased to 25kPa at a time interval of 60 s to examine if any oil droplet appeared on the membrane surface. The pressure was noted when the oil droplets appear on the membrane surface. The experiment was carried out three times using three different set of membranes made from the same condition. The results were averaged to obtain the final LEP_{oil}.

2.7 Clean Water Permeability experiment

The clean water flux of the control PES and the PES-G-PANCMI membranes were measured using similar setup used in our previous study (Prince et al., 2014). The fibers with the total effective membrane area of 90 cm^2 (10 fibers and 30 cm length (effective length 24cm)) were used to fabricate the membrane module. The two edges of the membrane module were sealed by using epoxy glue while keeping the lumen open on one side to collect the clean water. The developed membrane module was mounted to the filtration system. Cross-flow ultrafiltration experiments (out to in) were carried out by using a filtration system at a constant feed pressure of 1bar. To evaluate the performance of the prepared membrane in oil water separation, a long time (8 hrs) filtration test was carried out using 200ppm oil (oil emulsion) in DI water at the same condition for both control PES membrane and the modified PES-G-PANCMI membrane individually.

3.Results and Discussion

3.1. Structural analysis

The structure of the PES, G-PANCMI and PES/G-PANCMI membranes were confirmed using Fourier Transform Infra Red Spectroscopy (FTIR) as shown in **Fig.5**. The FTIR spectra of PES membrane showed a peak for the C-H stretching peak of benzene ring at 2974 cm^{-1}. Three peaks

between 1600 $cm^{-1}$and 1400 cm^{-1}were attributed to aromatic ring vibration. The C-O-C stretching peaks were located at 1320 $cm^{-1}$and 1233 cm^{-1}. The S=O stretching peaks were present at 1150 $cm^{-1}$and 1102 cm^{-1}. The FTIR spectrum of G-PANCMI showed a broad band at 3219cm^{-1} corresponding to the –NH stretching vibration of the diamine moiety, a small peak at 2931cm^{-1} for the –CH stretching vibration, a sharp peak at 2245cm^{-1} corresponding to the –CN stretching vibration of the nitrile group and two sharp peaks at 1770cm^{-1} and 1718cm^{-1}correspondingto the C=O stretching vibrations of the imide carbonyl groups and finally a peak at 1386cm^{-1} for –C-N-C stretching vibration confirming the formation of imide functionality by the attachment of amine modified xGnP to PANCMA. The FTIR spectra of PES/G-PANCMI membrane showed the presence of both PES and G-PANCMI peaks confirming the successful incorporation of G-PANCMI in PES matrix.

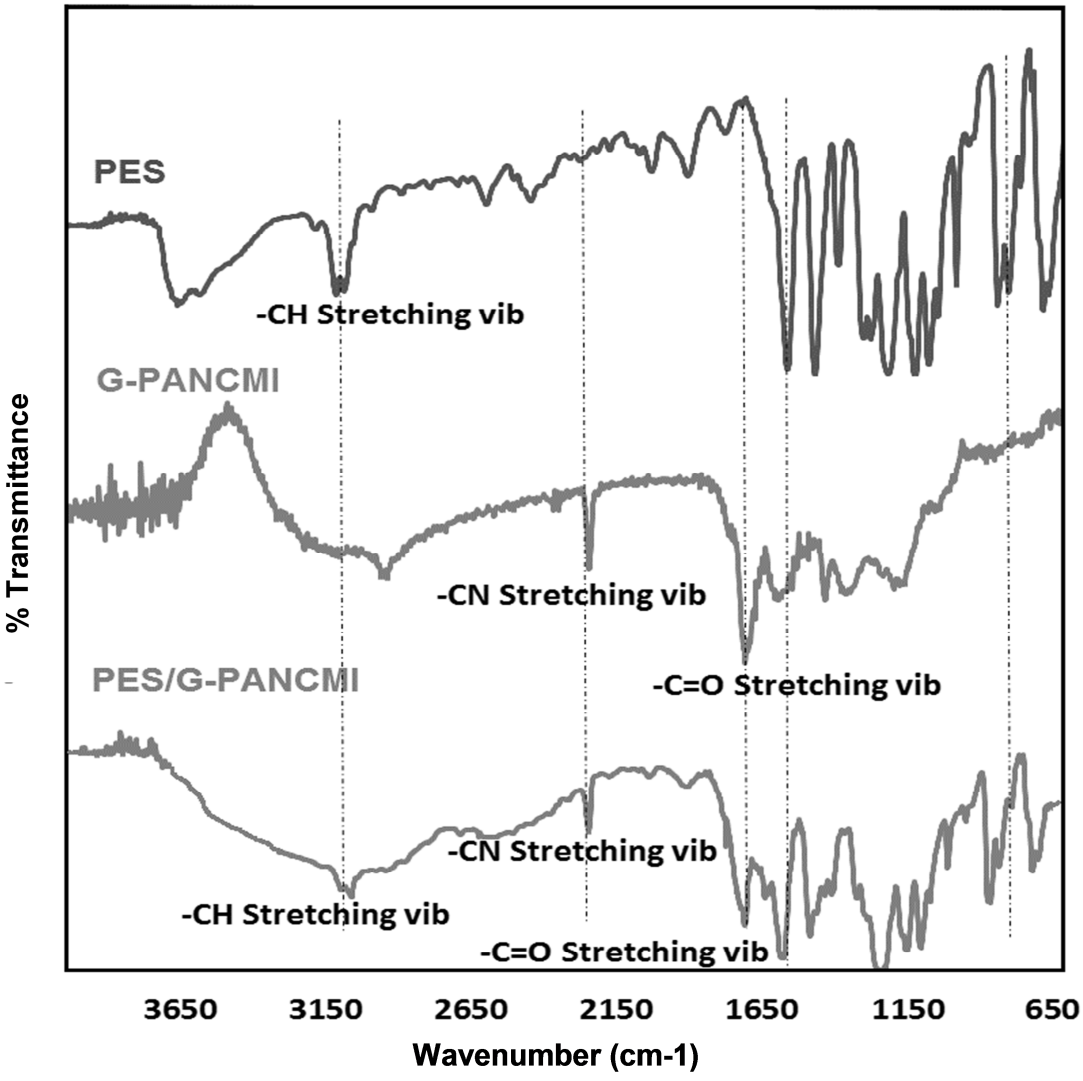

Fig. 5. FTIR spectra of the control PES, G-PANCMI and the modified membrane PES-G-PANCMI

3.2 Mechanical and Thermal analysis

Thermo gravimetric (TG) analysis was performed to investigate the effect of incorporation of the novel ultra-wetting graphene (G-PANCMI) on the thermal property of the PES UF membranes. The differences in thermal stability of PES and PES-G-PANCMI based membranes are highlighted in **Fig. 6 (a)**. Compared to PES membrane, PES-G-PANCMI membrane showed excellent thermal stability. The drastic weight loss for PES started at about 180°C. Whereas, PES-G-PANCMI showed greater thermal stability up to a temperature of 210°C, without much weight loss confirming the improved thermal properties of the PES due to the presence of G-PANCMI in the membrane matrix.

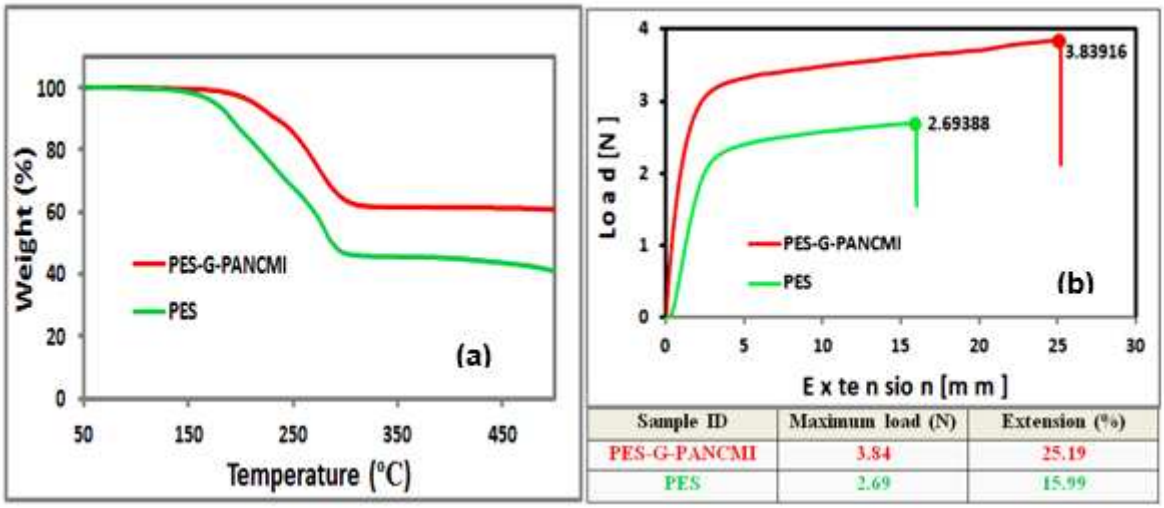

Sample ID	Maximum load (N)	Extension (%)
PES-G-PANCMI	3.84	25.19
PES	2.69	15.99

Fig. 6. (a) Thermo gravimetric (TG) analysis and (b) the mechanical property of the control PES and the modified membrane PES-G-PANCMI

The mechanical property of the control PES and the modified PES-G-PANCMI membranes were studied using an Instron universal testing machine and the results are presented in **Fig.6 (b).** Compared to PES membrane, PES-G-PANCMI membrane showed excellent mechanical stability. The maximum load achieved for the PES membrane was 2.69 N whereas, PES-G-PANCMI showed greater mechanical stability of 3.84 N which is around 30% higher than the PES membrane.

Similarly, the elongation (extension) of the PES-G-PANCMI membrane (25%) was also higher compared to PES membrane (15%). The improved mechanical properties of the PES UF membrane is due to the presence of G-PANCMI in the membrane matrix.

3.3 Morphological analysis

The surface morphology and cross section of the PES and ultra-wetting graphene modified PES-G-PANCMI based hollow fibre membranes were examined using SEM and the pictures are presented in **Fig.7,** (a) cross section, (b) outer surface and (c) actual image. Both membranes had an average inner diameter of 0.6mm and an outer diameter of 1.2mm. However, the hollow fibre membranes exhibit different internal structures depending on their composition. The internal structure of PES membrane has a large number of macro voids. Whereas, the ultra-wetting graphene modified PES-G-PANCMI membranes has a lower macro voids with more sponge like structures in the cross section next to the internal surface. This is due to the increase in viscosity and the coagulation value of the casting solution. Further, G-PANCMI contains highly hydrophilic amine and carboxylic groups which slows down the non solvent/solvent exchange. As a result less water was drawn into the membrane which lead to the sponge like structure. Sponge like structure helps to enhance the water permeability and selectivity. In addition to that, the even distribution of ultra-wetting graphene nano sheets can be identified in the cross section and on the outer surface of the PES-G-PANCMI modified membrane.

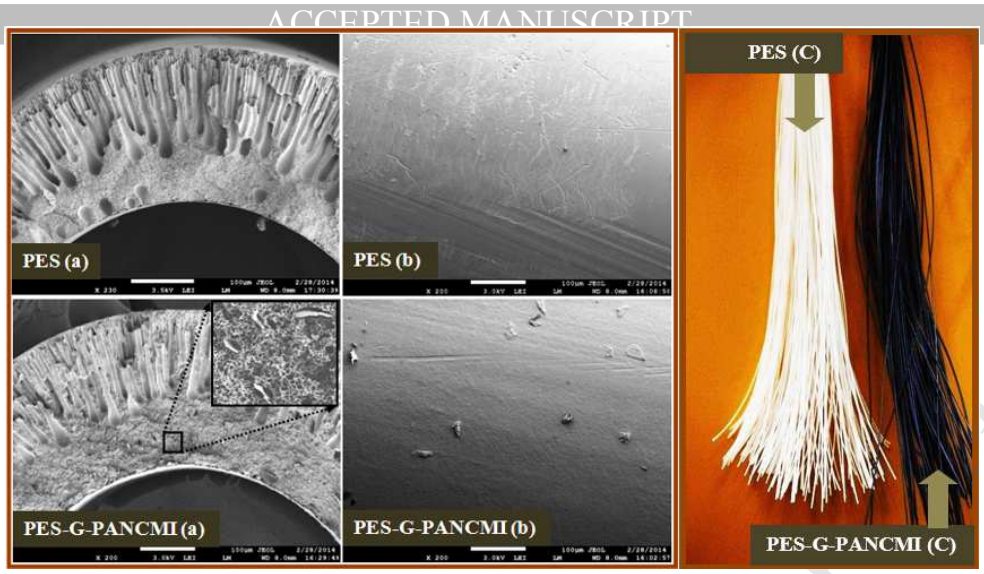

Fig. 7. SEM images of PES and PES-G-PANCMI membranes (a) Cross section (b) Outer surface (c) Actual image of synthesized PES and PES-G-PANCMA membranes

3.4 Pore size analysis

Pore size analysis: The average pore size of the PES membrane and the ultra-wetting graphene modified PES-G-PANCMI membranes were measured and the experimental data indicated that there is no significant difference on the mean pore size of both PES and PES-G-PANCMI membranes. The average pore sizes of PES membrane was 0.07 ± 0.02µm and 0.07 ± 0.03µm for the PES-G-PANCMI membrane.

3.5 Performance analysis

Fig. 8 (a) shows average LEP_{oil} of the membranes together with its error range. Comparing the LEP_{oil}, even though the membrane pore size was almost same for PES and G-PANCMI, LEP_{oil} increased from 50±10kPa of PES membrane to 175± 25kPa of PES-G-PANCMI membrane (with ultra-wetting graphene), which is 350% (3.5 times) higher than the PES membrane.

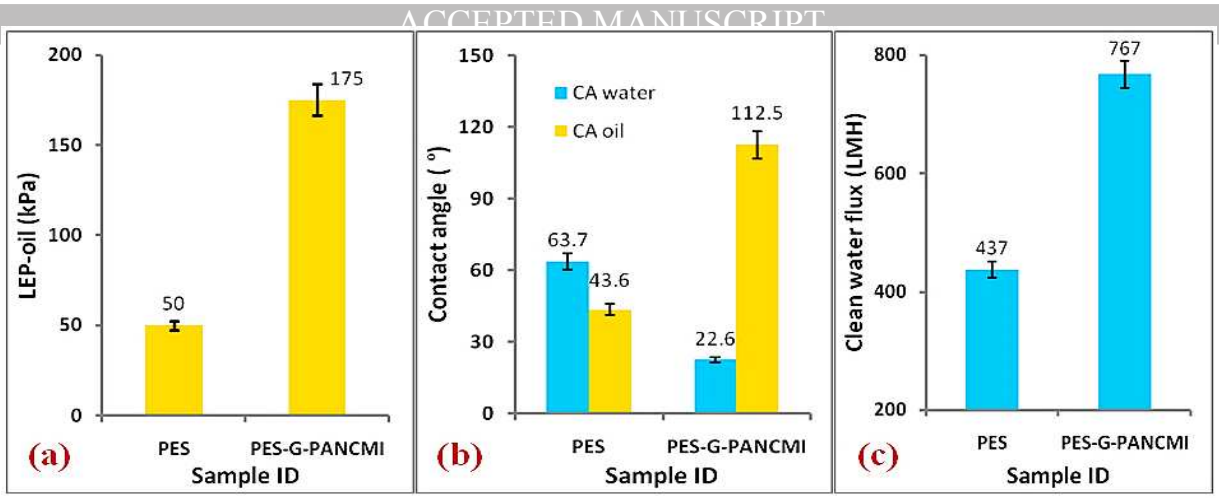

Fig.8. (a) Liquid entry pressure of oil (LEP_{oil}) analysis, (b) Water and oil contact angle and (c) Clean water flux of the PES and PES-G-PANCMI membrane samples

The increase in LEP_{oil} thus parallels to the increase in oil (dichloroethane) contact angle (oleophobicity) of the ultra-wetting graphene modified PES-G-PANCMI membrane. The oleophobicity of the PES membrane and PES-G-PANCMI membranes were measured by their oil contact angle by using dichloroethane and the results are presented in **Fig. 8 (b).** The PES membrane sample showed an oil contact angle of 43.6 ± 3.5^o. Ultra-wetting graphene modified PES-G-PANCMI membrane sample showed an oil contact angle of 112.5 ± 3.2^o which is 158% higher compared to that of the PES membrane. Similarly, the hydrophilicity of the PES membrane and PES-G-PANCMI membranes were measured by their water contact angle and the results are presented **in Fig.8 (b).** The PES membrane sample showed a water contact angle of 63.7± 3.8^o. Ultra-wetting graphene modified PES-G-PANCMI based membrane sample showed a water contact angle of 22.6± 2.5^o which is 64.5% reduction compared to that of the PES membrane sample. The effectiveness of the ultra-wetting graphene on the hydrophilicity is clearly demonstrated by these tests. The increased hydrophilicity is attributed to the presence of the amine (-NH_2) and acid (-COOH) groups attached to the nano graphene sheets in the G-PANCMI matrix of the PES-G-PANCMI membrane.

The prepared PES membrane and the ultra-wetting graphene modified PES-G-PANCMI ultrafiltration membrane were tested to evaluate the clean water flux of the membrane using a cross flow filtration method. **Fig.8 (c)** shows the clean water flux for both membranes at a constant feed

water pressure of 100 kPa (1bar). The PES membrane gave a pure water flux of 437± 18 LMH. Even though the pore size are similar for both membrane, the ultra-wetting graphene modified PES-G-PANCMI based membrane gave higher pure water flux of 767± 23 LMH which is around 43% higher compared to the PES based membrane. This increase in pure water flux is due to the increase in hydrophilicity / wettability of the membrane.

To evaluate the performance of the prepared membrane in oil water separation, a long time (8 hrs) filtration test was conducted using 200ppm oil emulsion (oil emulsion was kept at constant stirring at 400rpm during filtration in order to have a homogeneous emulsion) in DI water for the control PES membrane and the PES-G-PANCMI membrane individually, and the results are summarized in **Fig. 9.** It is observed that the ultra-wetting graphene modified PES-G-PANCMI membrane gives stable flux compared to PES based membrane. The flux drop for the PES-G-PANCMI membrane is only 9.2% (<10) of the initial flux after 8 hrs oil emulsion in water separation whereas the PES membrane's flux drop is 65% for the same duration of operation. The obtained results highlight that the presence of G-PANCMI helps to reduce fouling (oil deposition) on the membrane surface. The reduced oil adhesion is mainly due to the presence highly hydrophilic amine ($-NH_2$) and acid (-COOH) groups attached to the nano graphene sheets in the G-PANCMI matrix (Prince et al., 2016)of the PES-G-PANCMI membrane Previous literature studies also indicate similar effects on the oil separation efficiency of the hydrophilic membranes (Xu et al., 2013, Tian et al., 2012,Wen et al., 2013,Xue et al., 2011)

In order to evaluate the oil-emulsion selectivity of the membrane, the total organic carbon (TOC) of the feed (oil-emulsified solution) and permeate were measured every hour. Percentage of oil emulsion rejection (selectivity) was calculated and presented in **Fig. 9 (b)**. From the data, it is found that the selectivity for the PES-G-PANCMI membrane is higher and stable compared to the control PES membrane. The selectivity for control PES membrane drops over time which may be due to change in surface properties of the membrane over time. These result further confirms the increased hydrophilicity of the PES membranes by G-PANCMI. Based on our findings, we conclude that the

ultra-wetting graphene offers the distinct potential to be an ideal material with significantly improved properties for new generation water filtration membranes.

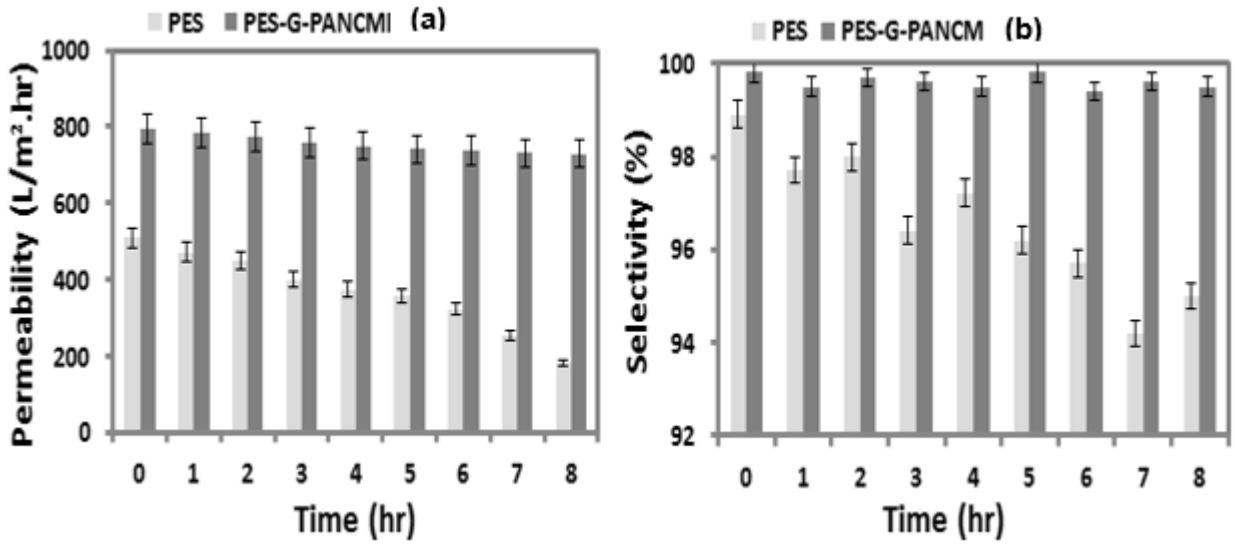

Fig. 9: (a) Permeability (flux drop) and (b) oil removal efficiency of the membrane samples PES & PES-G-PANCMI in a long time study of 8 hrs

4. Conclusions

In this work, a simple method to increase the hydrophilicity of the PES hollow fibre UF membrane by using hydrophilic functionalised graphene grafted poly acrylonitrile-co-maleimide (G-PANCMI) or ultra-wetting graphene for successful oil-water separation has been investigated. The prepared membranes were characterized thoroughly and the experimental data indicates that the G-PANCMI play an important role in enhancing the hydrophilicity/wettability, water permeability and selectivity of the PES UF membrane. The water contact angle (CA_w) of the PES membrane is reduced from 63.7 ± 3.8^o to 22.6 ± 2.5^o which is 64.5% reduction while, the oil contact angle was increased from 43.6 ± 3.5^o to 112.5± 3.2^o which is 158% higher compared to that of the PES membrane. Similarly, the LEP_{oil} increased 350% from 50±10 kPa of the control PES membrane to 175± 25 kPa of PES-G-PANCMI membrane. More importantly, the water permeability increased by 43% with >99% selectivity. Based on our findings we conclude that the development of PES-G-PANCMI membrane will create a new avenue for successful oil-water separation

Acknowledgements

This work was supported from funding provided by Ministry of Education, Singapore under the Innovation Fund. The authors also gratefully acknowledge the support from Newcastle University, United Kingdom and Environmental & Water Technology Centre of Innovation (EWTCOI), Ngee Ann Polytechnic, Singapore for the NU-Poly-SIT scholarship to J.A.P.

References

Akin, I., Zor, E., Bingol, H. & Ersoz, M. 2014. Green Synthesis of Reduced Graphene Oxide/Polyaniline Composite and Its Application for Salt Rejection by Polysulfone-Based Composite Membranes. The Journal of Physical Chemistry B 118, 5707-5716.

Chen, P.-C. & Xu, Z.-K. 2013. Mineral-Coated Polymer Membranes with Superhydrophilicity and Underwater Superoleophobicity for Effective Oil/Water Separation. Sci. Rep. 3.

Cheryan, M. & Rajagopalan, N. 1998. Membrane processing of oily streams. Wastewater treatment and waste reduction. Journal of Membrane Science **151**, 13-28.

Deng, D. 2013. Hydrophobic Meshes for Oil Spill Recovery Devices. ACS Applied Materials & Interfaces **5**, 774-781.

Duan, W. 2014. Electrochemical mineral scale prevention and removal on electrically conducting carbon nanotube--polyamide reverse osmosis membranes. Environmental science. Processes & impacts 16, 1300-1308.

Feng, L. 2004. A super-hydrophobic and super-oleophilic coating mesh film for the separation of oil and water. Angewandte Chemie (International ed. in English) 43, 2012-2014.

Gai, J.-G., Gong, X.-L., Wang, W.-W., Zhang, X. & Kang, W.-L. 2014. An ultrafast water transport forward osmosis membrane: porous graphene. Journal of Materials Chemistry A 2, 4023-4028.

Group, W. B. 1998. Pollution prevention and abatement handbook. World Bank Group.

Han, Y., Xu, Z. & Gao, C. 2013. Ultrathin Graphene Nanofiltration Membrane for Water Purification. Advanced Functional Materials 23, 3693-3700.

Heo, Y., Im, H. & Kim, J. 2013. The effect of sulfonated graphene oxide on Sulfonated Poly (Ether Ether Ketone) membrane for direct methanol fuel cells. Journal of Membrane Science 425–426, 11-22.

Jin, F. 2013. High-performance ultrafiltration membranes based on polyethersulfone-graphene oxide composites. RSC Advances 3, 21394-21397.

Kota, A. K., Kwon, G., Choi, W., Mabry, J. M. & Tuteja, A. 2012. Hygro-responsive membranes for effective oil–water separation. Nat Commun 3, 1025.

Li, D., Muller, M. B., Gilje, S., Kaner, R. B. & Wallace, G. G. 2008. Processable aqueous dispersions of graphene nanosheets. Nat Nano 3, 101-105.

Lu, P. 2009. Macroporous silicon oxycarbide fibres with luffa-like superhydrophobic shells. J Am Chem Soc 131, 10346-10347.

Nordvik, A. B., Simmons, J. L., Bitting, K. R., Lewis, A. & Strøm-Kristiansen, T. 1996. Oil and water separation in marine oil spill clean-up operations. Spill Science & Technology Bulletin **3**, 107-122.

Novoselov, K. S. 2004. Electric Field Effect in Atomically Thin Carbon Films. Science 306, 666-669.

Prince, J. A., Bhuvana, S., Anbharasi, V., Ayyanar, N., Boodhoo, K. V. K., & Singh, G. 2016. Ultra-wetting graphene based membrane. Journal of Membrane Science 500, 76-85**.**

Prince, J. A., Bhuvana, S., Boodhoo, K. V. K., Anbharasi, V. & Singh, G. 2014. Synthesis and characterization of PEG-Ag immobilized PES hollow fiber ultrafiltration membranes with long lasting antifouling properties. Journal of Membrane Science 454, 538-548.

Reilly, W., O'Farrell, T. & Rubin, M. . Development Document for 1991 Proposed Effluent Limitation Guidelines and New Source Performance Standards for the Offshore Subcategory of the Oil and Gas Extraction Point Source Category. US Environ. Prot. Agency .

Samuel J. Maguire-Boyle, Andrew R. Barron. 2011. A new functionalization strategy for oil/water separation membranes, Journal of Membrane Science 382, 107-115.

Shannon, M. A. 2008. Science and technology for water purification in the coming decades. Nature 452, 301-310.

Shi, Z. 2013. Ultrafast separation of emulsified oil/water mixtures by ultrathin free-standing single-walled carbon nanotube network films. *Advanced materials (Deerfield Beach, Fla.)* **25**, 2422-2427.

Sirivedhin, T. & Dallbauman, L. 2004. Organic matrix in produced water from the Osage-Skiatook Petroleum Environmental Research site, Osage county, Oklahoma. Chemosphere 57, 463-469.

Sun, P. 2013. Selective Ion Penetration of Graphene Oxide Membranes. ACS nano 7, 428-437.

Tasaki, K., Gasa, J., Wang, H. & DeSousa, R. 2007. Fabrication and characterization of fullerene–Nafion composite membranes. Polymer 48, 4438-4448.

Tian, D. 2012. Photo-induced water-oil separation based on switchable superhydrophobicity-superhydrophilicity and underwater superoleophobicity of the aligned ZnO nanorod array-coated mesh films. Journal of Materials Chemistry 22, 19652-19657.

Wen, Q., Di, J., Jiang, L., Yu, J. & Xu, R. 2013. Zeolite-coated mesh film for efficient oil-water separation. Chemical Science 4, 591-595.

Xu, L. P. 2013. An ion-induced low-oil-adhesion organic/inorganic hybrid film for stable superoleophobicity in seawater. Advanced materials (Deerfield Beach, Fla.) 25, 606-611.

Xue, Z. 2011. A novel superhydrophilic and underwater superoleophobic hydrogel-coated mesh for oil/water separation. Advanced materials (Deerfield Beach, Fla.) 23, 4270-4273.

Zhang, J. & Seeger, S. 2011. Polyester Materials with Superwetting Silicone Nanofilaments for Oil/Water Separation and Selective Oil Absorption. Advanced Functional Materials 21, 4699-4704.

Zhang, W. 2013. Superhydrophobic and superoleophilic PVDF membranes for effective separation of water-in-oil emulsions with high flux. Advanced materials (Deerfield Beach, Fla.) 25, 2071-2076.

Zhang, L., Zhong, Y., Cha, D. & Wang, P. A. 2013. self-cleaning underwater superoleophobic mesh for oil-water separation. Sci. Rep. 3.

Zhang, L., Zhang, Z. & Wang, P. 2012. Smart surfaces with switchable superoleophilicity and superoleophobicity in aqueous media: toward controllable oil/water separation. NPG Asia Mater 4, e8.

Zhao, Y. 2013. Effect of graphite oxide and multi-walled carbon nanotubes on the microstructure and performance of PVDF membranes. Separation and Purification Technology 103, 78-83.

Zhu, Y. 2013. A novel zwitterionic polyelectrolyte grafted PVDF membrane for thoroughly separating oil from water with ultrahigh efficiency. Journal of Materials Chemistry A 1, 5758-5765.

Zinadini, S., Zinatizadeh, A. A., Rahimi, M., Vatanpour, V. & Zangeneh, H. 2014. Preparation of a novel antifouling mixed matrix PES membrane by embedding graphene oxide nanoplates. Journal of Membrane Science 453, 292-301.

Highlights

1. A new water insoluble highly hydrophilic copolymer PANCMACDAMN was developed.
2. Ultra-wetting graphene additive was used to fabricate PES hollow fiber membranes.
3. The new copolymer additive increases the hydrophilicity of the membrane by 64.5%
4. The addition of 5% ultra-wetting graphene increase the LEP_{oil} of the PES membrane by 350%
5. The permeability of the membrane was increased by 43% with the new ultra-wetting graphene